Protocatechuic Acid and Syringin from *Saussurea neoserrata* Nakai Attenuate Prostaglandin Production in Keratinocytes Exposed to Airborne Particulate Matter

Myeongguk Jeong , Yeongdon Ju , Hyukjin Kwon , Yeeun Kim , Kyung-ye Hyun * , Go-Eun Choi *

Posted Date: 25 June 2023

doi: 10.20944/preprints202306.1713.v1

Keywords: Saussurea neoserrata Nakai; preparative liquid chromatography; particulate matter; antioxidant; protocatechuic acid; syringin

Article

Protocatechuic Acid and Syringin from *Saussurea neoserrata* Nakai Attenuate Prostaglandin Production in Keratinocytes Exposed to Airborne Particulate Matter

Myeongguk Jeong[1†], Yeongdon Ju[1,2†], Hyukjin Kwon[1], Yeeun Kim[1], Kyung-ye Hyun[3*] and Go-Eun Choi[1*]

[1] Department of Biomedical Laboratory Science, College of Health Sciences, Catholic University of Pusan, Busan 46252, Korea; audrnr04@gmail.com
[2] Medical Science Research Center, Pusan National University, Yangsan, 50612, Korea; lrdrlr@naver.com
[3] Department of Clinical Laboratory Science, Dong-Eui University, Busan 47340, Korea; kyhyun@deu.ac.kr
* Correspondence: gechoi@cup.ac.kr (G.-E. C); kyhyun@deu.ac.kr (K.-Y. H.); Tel.: +82-51-510-0563 (G.-E. C); +82-51-890-2683 (K.-Y. H.)
† These authors contributed equally to this work.

Abstract: *Saussurea neoserrata* Nakai offers a reliable and efficient source of antioxidants that can help alleviate adverse skin reactions triggered by air pollutants. Air pollutants, such as particulate matter (PM), have the ability to infiltrate the skin and contribute to the higher occurrence of cardiovascular, cerebrovascular, and respiratory ailments. Individuals with compromised skin barriers are particularly susceptible to the impact of PM since it can be absorbed more readily through the skin. This study investigated the impact of protocatechuic acid and syringin, obtained from the n-BuOH extract of *S. neoserrata* Nakai, on the release of PGE_2 and PGD_2 induced by PM_{10}. Additionally, it examined the gene expression of enzymes involved in the synthesis of PGE_2 and PGD_2 in human keratinocytes. The findings of this research highlight the potential of utilizing safe and efficient plant-derived antioxidants in dermatological and cosmetic applications to mitigate the negative skin reactions caused by exposure to air pollution.

Keywords: *Saussurea neoserrata* Nakai; preparative liquid chromatography; particulate matter; antioxidant; protocatechuic acid; syringin

1. Introduction

According to the World Health Organization (WHO), air pollution is the most significant environmental health risk factor and, in 2018, it caused more than 4.2 million deaths (https://www.who.int). The primary air pollutants that pose severe health risks are particulate matter (PM), ozone (O3), nitrogen dioxide (NO2), and sulfur dioxide (SO2) [1]. Of these, Particulate matter (PM) is the leading cause of air pollution and consists of inorganic and organic solid and liquid particles suspended in the air [2]. PM_{10} and $PM_{2.5}$, with diameters less than 10 and 2.5 microns, respectively, can penetrate deeply into the lungs and bloodstream, increasing the risk of cardiovascular, cerebrovascular, and respiratory diseases [3-5].

The skin acts as a protective layer between the body and external pollutants, but harmful environmental pollutants can still affect it. Individuals with impaired skin barriers are more susceptible to PM due to increased absorption through the skin [6,7]. PM can even disrupt the skin's barrier function, further facilitating drug absorption [8]. The infiltration of PM into the skin can worsen skin conditions such as acne, atopic dermatitis, and psoriasis [9], as well as contribute to premature aging [10] and hyperpigmentation [11]. PM exposure in conjunction with UV rays can have a synergistic adverse effect on the skin, causing photoaging and even skin cancer [12,13].

Preprints (www.preprints.org) | NOT PEER-REVIEWED | Posted: 25 June 2023 doi:10.20944/preprints202306.1713.v1

Research has demonstrated that PM in the air can cause oxidative stress and inflammation by producing reactive oxygen species (ROS). Moreover, the activation of cytokines and matrix metalloproteinases can be induced in human dermal fibroblasts, epidermal keratinocytes and reconstructed epidermis models [14-17]. Furthermore, PM enhances the synthesis of the eicosanoid mediator prostaglandin (PG) E2 and diminishes the expression of filaggrin in human keratinocytes, resulting in impaired skin barrier function [18]. However, studies have demonstrated that eupafolin, derived from the medicinal plant phyla Nodiflora, can effectively hinder the expression of cyclooxygenase (COX)-2 and the production of PGE_2 in HaCaT keratinocytes when exposed to PM. Similarly, resveratrol, a polyphenol present in grapes and redwine, has also been observed to reduce PM-induced COX-2 expression and PGE_2 production in fibroblast-like synoviocytes, which are human cells with similarities to fibroblasts [19-22]. Therefore, the use of safe and effective antioxidants in dermatological and cosmetic approaches may help alleviate the negative skin reactions caused by PM exposure [23-25].

For thousands of years, plants have been the foundation of traditional medicine systems that continue to offer new remedies to humankind [26,27]. The genus *Saussurea* in the Asteraceae family is a large and diverse group of plants that has been widely used in traditional medicine for many purposes [28-30]. In Korea, the *Saussurea* genus is highly diverse with 32 recognized species, 16 of which are endemic [31]. In this study, we isolated protocatechuic acid and syringin from the n-BuOH extracts of *S. neoserrata* Nakai through fractionation. We investigated whether the extracts of *S. neoserrata* Nakai, as well as protocatechuic acid and syringin, could affect the release of PGE_2 and PGD_2 induced by PM_{10} and whether it could also affect the gene expression of the enzymes involved in PGE_2 and PGD_2 synthesis in human keratinocytes.

2. Materials and Methods

2.1. Materials and reagents

S. neoserrata Nakai was purchased from Daum International (Hanam, Korea) and immersed in distilled water at a sample-to-solvent ratio of 1:20 (w/v) for 24 h at 60 ℃. The mixtures were then homogenized at 60 ℃ for 4 h using a homogenizer (IKA, Staufen, Germany). The extracts were then filtered with filter paper, concentrated at 60 ℃ with a rotary evaporator (IKA, Staufen, Germany), and then freeze-dried for 24 h. All freeze-dried extracts were stored at 4 ℃ prior to further experiments. All experiments were repeated in triplicate. LC-Forte/R preparative **l**iquid **c**hromatography (prep-LC) (YMC, Kyoto, Japan) was carried out using **a** YMC-DispoPack cartridge (ODS, 30 g) (YMC, Kyoto, Japan). Silica gel (230-400 mesh) (Merck, Darmstadt, Germany), Kromasil 100-5-C18 (Nouryon, Bohus, Sweden), and Sephadex LH-20 (Merck, Darmstadt, Germany) were used for the column chromatography. Thin-layer chromatography (TLC) analysis was performed on a Kiesel gel 60 F254 plate (Merck, Darmastdt, Germany) and RP-18 F254s plates (Merck, Darmastdt, Germany); detection was performed via spraying and heating with a UV lamp at 254 nm and 356 nm in a 10% H2SO4 solution. The 1H, 13C NMR, and 2D NMR spectra were recorded on a Bruker AVANCE II 400 (400 MHz for 1H NMR and 100 MHz for 13C NMR) spectrometer (Bruker, Bremen, Germany) in pyridine-d5 with TMS as the internal standard. ESI/MS was obtained on a 6530 Accurate-Mass Q-TOF LC/MS (Agilent Technologies, Waldbronn, Germany). All chemicals were reagent grade and purchased from Sigma Chemical Co. (MO, USA).

2.2. Extraction and isolation

The freeze-dried extract was partitioned with water, EtOAc, and n-BuOH in order to obtain the EtOAc (530 mg), n-BuOH (2.1 g), and H_2O extracts (32.6 g). The n-BuOH extract (2.1 g) was fractioned in a Kromasil column using silica gel (12 cm x 14 cm i.d.) as the adsorbent and eluted with gradients of CHCl3–MeOH (1:9, v/v) to afford six fractions. Fraction 2 (82 mg) was chromatographed on a Kromasil column with silica gel as the adsorbent and was successively eluted with gradients of $CHCl_3$–MeOH (0.5:9.5, v/v) to afford two fractions. Fraction 2-1-1 was purified repeatedly over a Sephadex LH-20 column with a mixture of CHCl3–MeOH (1:9, v/v) to acquire the compound (10.4

Preprints (www.preprints.org) | NOT PEER-REVIEWED | Posted: 25 June 2023 doi:10.20944/preprints202306.1713.v1

mg). Fraction 3 (77 mg) was followed by prep-LC using a YMC-DispoPack cartridge. These fractions were analyzed with a UV detector at 254 nm and 356 nm, whereby the mobile phase consisted of A: 0.1% formic acid in water and B: 0.1% formic acid in acetonitrile, with a flow rate of 0.4 mL/min. A flow chart of the entire extraction process is shown in Figure 1. Bold squares represent the fraction for which each single compound was identified using NMR spectra.

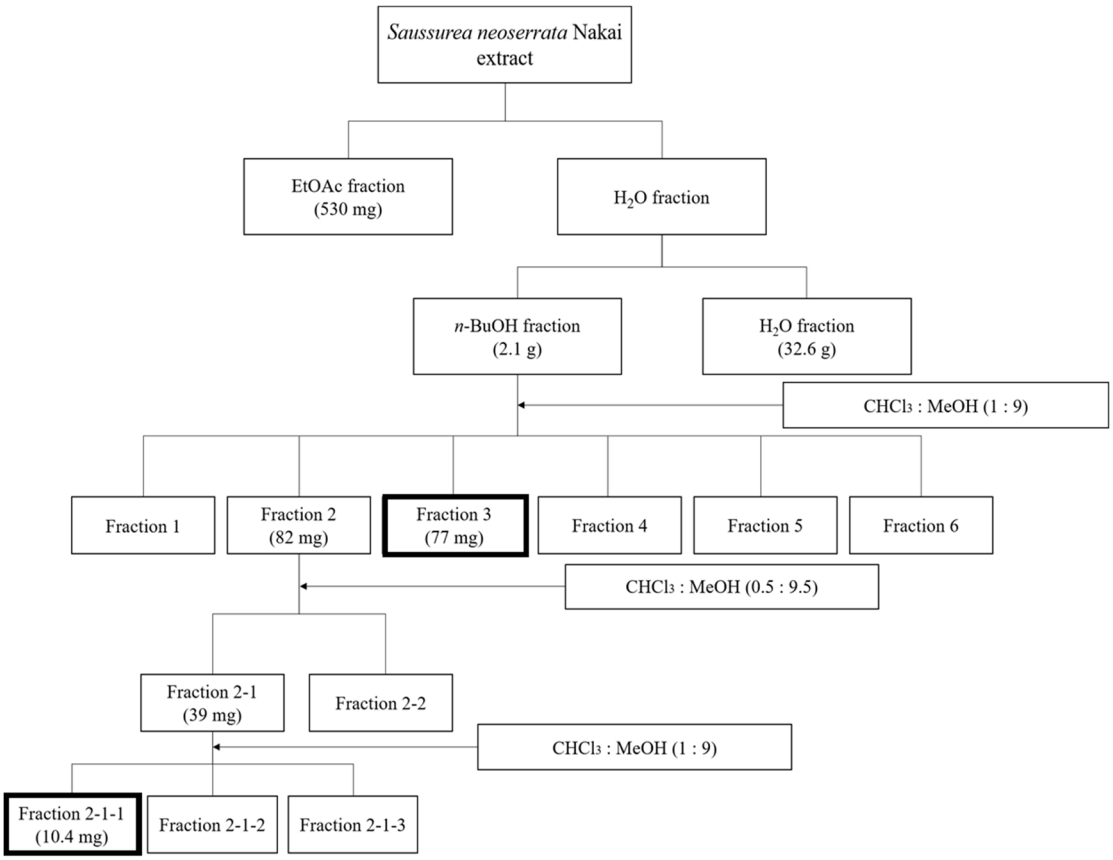

Figure 1. Schematic representation of the extraction and fractionation process of *S. neoserrata* Nakai.

2.3. Cell Culture

HaCaT cells—an immortalized human keratinocyte cell line established by Norbert E. Fusenig and named so as to denote its origin from human adult skin keratinocytes that were propagated under low Ca^{2+} conditions and elevated temperatures—were obtained from In-San Kim (Kyungpook National University, Daegu, Korea). The cells were cultured in a closed incubator at 37 ℃ in humidified air containing 5% CO_2. Cells were grown in DMEM/F-12 medium (GIBCO, Paisley, UK) containing 10% fetal bovine serum, 100 U/mL penicillin, 100 μg/mL streptomycin, 0.25 μg/mL amphotericin B, and 10 μg/mL hydrocortisone and passaged every three days.

2.4. Treatment of Cells with PM_{10}

The cells were seeded onto 6-well culture plates (SPL Life Sciences, Pocheon, Korea) at density 8×10^4 cells/well and incubated in a growth medium for 24 h. Prior to each experiment, a standardized PM_{10}-like fine dust (European Reference Material ERM-CZ120PM10) (Sigma Chemical Co., Mo, USA) was suspended in phosphate-buffered saline (PBS) at a suitable concentration for each specific treatment. The cells were exposed to PM_{10} at various concentrations ranging from 6.25 to 100 μg/mL for 24 to 48 h, depending on the specific objective of the experiment. Additionally, the cells were treated with specified concentrations of *S. neoserrata* Nakai extract or dieckol, either in combination

Preprints (www.preprints.org) | NOT PEER-REVIEWED | Posted: 25 June 2023 doi:10.20944/preprints202306.1713.v1

with PM_{10} or separately. To assess antioxidant effects, N-acetyl cysteine (NAC) (Sigma Chemical Co., MO, USA) was utilized as a positive control.

2.5. Cell Viability Assay

Cell viability was evaluated using a 3-[4,5-dimethylthiazol-2-yl]-2,5-diphenyl tetrazolium bromide (MTT) assay. The cells were cultured in 200 μL of growth medium containing 1 mg/mL MTT (Amresco, OH, USA) for 2 h at room temperature. Following the removal of the medium, the formazan crystals were dissolved in 200 μL of dimethyl sulfoxide (DMSO) and the absorbances measured at 595 nm with a SPECTROstar Nano microplate reader (BMG LABTECH GmbH, Ortenberg, Germany).

2.6. Enzyme-Linked Immunosorbent Assay (ELISA)

The concentration of PGE_2 protein in the culture medium waw measured by employing an ELISA kit specifically designed for detecting prostaglandin E_2 (Cayman Chemical Co., MI, USA). In this particular assay, a predetermined quantity of PGE_2–acetylcholinesterase (AChE) conjugate is employed as a tracer for PGE_2. The binding of this conjugate to a monoclonal antibody against PGE_2 is inversely related to the amount of PGE_2 present in the sample being analyzed. Briefly, 50 μL of cell culture medium diluted four times or standard PGE_2 solutions were carefully placed into microplate wells already containing immobilized goat polyclonal anti-mouse IgG. PGE_2 tracers and PGE_2 monoclonal antibodies were added to each well, and the mixtures were allowed to incubate at 4 ℃ for 18 h. The wells were subsequently washed five times using a wash buffer. Then, the AChE reaction was initiated by introducing Ellman's reagent, composed of acetylthiocholine and 5,50-dithio-bis-(2-nitrobenzoic acid), into the solution. Following a 60 min incubation period, the absorbances were recorded at 405 nm using a SPECTROstar Nano microplate reader (BMG LABTECH GmbH, Ortenberg, Germany). The concentration of PGE_2 was estimated using a standard curve.

2.7. Assay for Cellular ROS Production

Next, 2′,7′-dichlorofluorescein diacetate (DCFH-DA) (Sigma Chemical Co., MO, USA) was used as a fluorescent probe for measuring the changes in intracellular active oxygen concentration. DCFH-DA, a non-fluorescent substance, emits green fluorescence when oxidized by ROS and can therefore be used to measure ROS levels. For this, HaCaT cells were inoculated into a 60 mm culture dish and cultured for 24 hours. After treatment with the samples and H_2O_2, cells were incubated for 2 hours. Before harvesting, 10 μM DCFH-DA was applied to the cell culture medium and incubation continued for 30 min. The cells were then washed with PBS, harvested with a 1% trypsin–EDTA solution, and washed again with PBS. The change in ROS levels (green fluorescence) was measured using a flow cytometer (Becton Dickinson, OR, USA).

2.8. Quantitative Reverse Transcription Polymerase Chain Reaction (qRT-PCR) Analysis

The mRNA levels of COX-1, COX-2, microsomal prostaglandin E_2 synthase (mPGES)-1, mPGES-2, and cytosolic prostaglandin E_2 synthase (cPGES) were assessed using qRT-PCR with a StepOnePlus Real-Time PCR System (Applied Biosystems, CA, USA). Total RNA was extracted from the cells using an RNeasy kit (Qiagen, CA, USA), and used as a template for cDNA synthesis, employing a high-capacity cDNA archive kit (Applied Biosystems, CA, USA). The gene-specific primers for qRT-PCR analysis were obtained from Macrogen (Seoul, Korea), and their nucleotide sequences are presented in Table 1. The qRT-PCR reaction, a mixture of 20 μL was prepared, comprising a SYBR® Green PCR Master Mix (Applied Biosystems, CA, USA), cDNA (60 ng) and gene-specific primer sets (2 pmol). The thermal cycling parameters were set as follows: initial incubation at 50 °C for 2 min, followed by a denaturation step at 95 °C for 10 min, 40 amplification cycles of 95 °C for 15 s and 60

Preprints (www.preprints.org) | NOT PEER-REVIEWED | Posted: 25 June 2023 doi:10.20944/preprints202306.1713.v1

°C for 1 min, and a finally a dissociation step. Melting curve analysis was conducted in each run to confirm the homogeneity of the PCR product. The mRNA levels of each target gene were determined relative to the mRNA level of the internal reference, glyceraldehyde 3-phosphate dehydrogenase (GAPDH), using the comparative Ct method [37].

Table 1. Sequences of primers used for the quantitative reverse transcription polymerase chain reaction (qRT-PCR) of the gene transcripts.

Gene Name	GenBank Accession Number	Primer Sequences	Ref.
Cyclooxygenase 1 (COX-1)/Prostaglandin-endoperoxide synthase 1 (*PTGS1*)	NM_000962.4	Forward: 5'-CAGAGCCAGATGGCTGTGGG-3' Reverse: 5'-AAGCTGCTCATCGCCCCAGG-3'	[32]
Cyclooxygenase 2 (COX-2)/Prostaglandin-endoperoxide synthase 2 (*PTGS2*)	NM_000963.3	Forward: 5'-CTGCGCCTTTTCAAGGATGG-3' Reverse: 5'-CCCCACAGCAAACCGTAGAT-3'	[33]
Microsomal prostaglandin E synthase 1 (mPGES-1)/Prostaglandin E synthase (*PTGES*)	NM_004878.5	Forward: 5'-AACCCTTTTGTCGCCTG-3' Reverse: 5'-GTAGGCCACGGTGTGT-3'	[34]
Microsomal prostaglandin E synthase 2 (mPGES-2); Prostaglandin E synthase 2 (*PTGES2*)	NM_025072.7	Forward: 5'-GAAAGCTCGCAACAACTAAAT-3' Reverse: 5'-CTTCATGGCTGGGTAGTAG-3'	[34]
Cytosolic prostaglandin E synthase (cPGES)/ Prostaglandin E synthase 3 (*PTGES3*)	NM_006601.6	Forward: 5′-ATAAAAGAACGGACAGATCAA-3′ Reverse: 5′-CACTAAGCCAATTAAGCTTTG-3′	[34]
L-PGDS (*PTGDS*)	NM000954	Forward: 5'-AACCAGTGTGAGACCCGAAC-3' Reverse: 5'-AGGCGGTGAATTTCTCCTTT-3'	[35]
H-PGDS (*HPGDS*)	NM014485	Forward: 5'-CCCCATTTTGGAAGTTGATG-3' Reverse: 5'-TGAGGCGCATTATACGTGAG-3	[35]
GAPDH (glyceraldehyde 3-phosphate dehydrogenase)	NM_002046.3	Forward: 5'-ATGGGGAAGGTGAAGGTCG-3' Reverse: 5'-GGGGTCATTGATGGCAACAA-3'	[36]

2.9. Statistical Analysis

The data are presented as the mean ± standard deviation (SD) obtained from three or more independent experiments. Statistical analysis was performed using SigmaStat v.3.11 software (Systat Software Inc., CA, USA) with one-way analysis of variance (ANOVA). Subsequently, Dunnett's test was employed to compare all treatment groups against a single control group. A p-value below 0.05 was considered statistically significant.

Preprints (www.preprints.org) | NOT PEER-REVIEWED | Posted: 25 June 2023 doi:10.20944/preprints202306.1713.v1

3. Results

3.1. Purification of protocatechuic acid from S. neoserrata Nakai

In the ^{1}H-NMR spectrum, δ_H 7.46 (1H, br.s, H-2), δ_H 7.44 (1H, dd, J = 8.0, 2.0 Hz, H-6), δ_H 6.81 (1H, d, J = 8.0 Hz, In H-5), and three olefin methine proton signals were identified. Through this, the existence of a 1,3,4 trisubstituted benzene ring was predicted.

Seven carbon signals were identified in the ^{13}C-NMR spectrum. Carbonyl carbon was confirmed in the signals of δ_C 170.8 (C-7), δ_C 151.3 (C-4), δ_C 145.9 (C-3), δ_C 124.0 (C-1), δ_C 123.9 (C-6), and δ_C 117.8 (C-5) Additionally, the presence of the 1,3,4-benzene ring was confirmed in the signal of δC 115.8 (C-2). Through this, the structure of the above compound 1 was determined as protocatechuic acid. ESI-MS was measured to confirm the molecular value. As a result, 153 $[M-H]^-$ was confirmed in negative mode, confirming the molecular weight of 154.

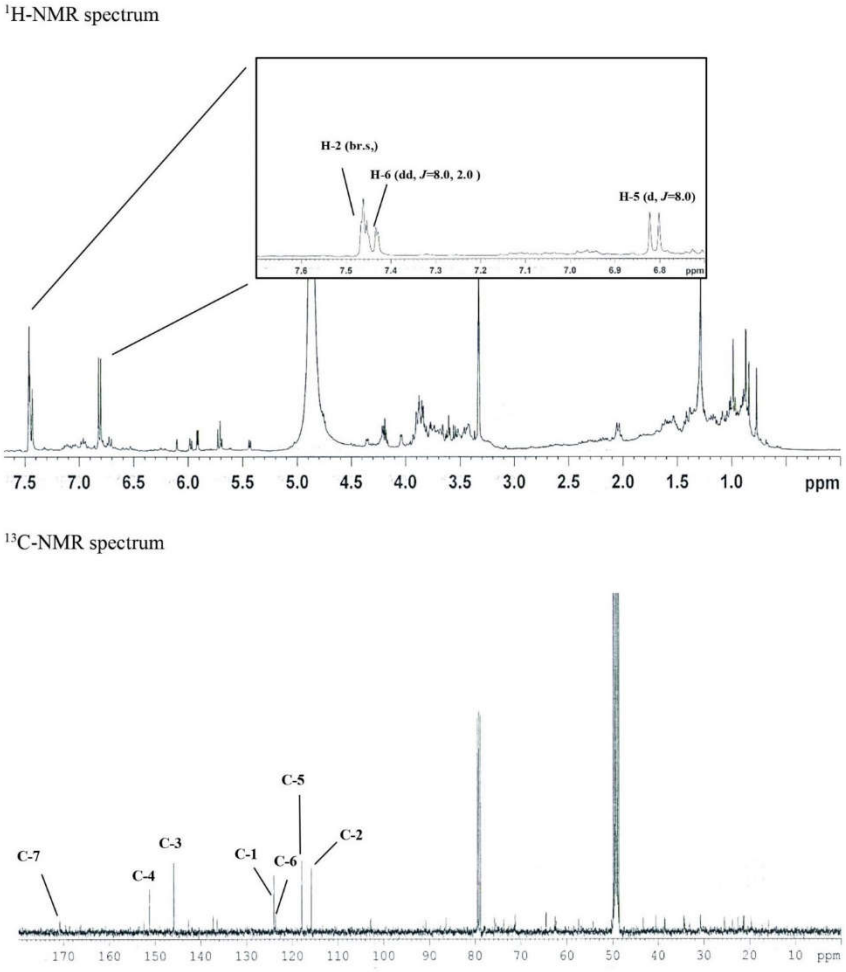

Figure 2. The ^{1}H-NMR and ^{13}C-NMR spectrum of Compound 1 (77 mg).

Preprints (www.preprints.org) | NOT PEER-REVIEWED | Posted: 25 June 2023 doi:10.20944/preprints202306.1713.v1

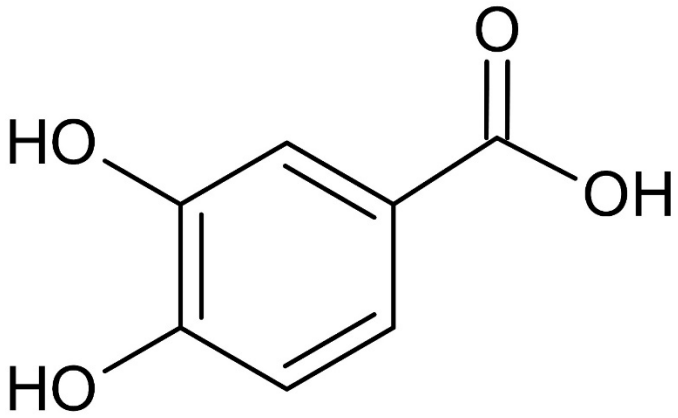

Figure 3. Chemical structure of the isolated protocatechuic acid ($C_7H_6O_4$) from *S. neoserrata* Nakai.

3.2. Purification of syringin from S. neoserrata Nakai

In the ^{1}H-NMR spectrum, δ_H 6.87 (2H, br.s, H-2,6), δ_H 6.86 (1H, d, *J* = 15.6 Hz, H-7), and δ_H 6.59 (1H, dt, *J* = 15.6, 4.8 Hz, H-8), as well as the presence of one symmetric tetra-substituted aromatic ring and one trans-double bond, were confirmed. One molecule per molecule at δ_H 5.79 (1H, d, *J* = 6.4 Hz, H-1') and an oxygenated methylene signal at δ_H 4.57 (1H, d, *J* = 3.8 Hz, H-9) and δ_H 3.74 (6H, s, H-OCH_3) confirmed the methoxy signal. Based on this, the above compound was expected to be an aromatic glycoside derivative.

In the ^{13}C-NMR spectrum, 17 carbon signals were identified, including one sugar molecule and two methoxy molecules. In the δ_C 154.3 (C-3,5) signal, oxygenated olefin quaternary carbon was confirmed and δ_C 136.4 (C-4).

One symmetric tetra-substituted aromatic ring and one trans-substituted ring in the presence of a double bond were confirmed. From the signal of δ_C 105.3 (C-1'), the anomer carbon originating from the sugar's carbon 1 was confirmed. In addition, δ_C 79.2 (C-3'), δ_C 78.8 (C-5'), δ_C 76.5 (C2'), and δ_C were obtained from the sugar moiety signal of 72.0 (C-4'). Moreover, for δ_C 63.0 (C-6'), the sugar structure was determined as glucose.

One oxygenated methylene and two methoxy molecules were identified through the signals of δ_C 63.2 (C-9) and δ_C 57.0 (C-OCH_3). Finally, the structure of this compound 2 was determined as syringin. To confirm the molecular value, ESI-MS was measured. As a result, 417 $[M-H+\text{formic acid}]^-$ was confirmed in negative mode, confirming the molecular weight of 372.

Preprints (www.preprints.org) | NOT PEER-REVIEWED | Posted: 25 June 2023 doi:10.20944/preprints202306.1713.v1

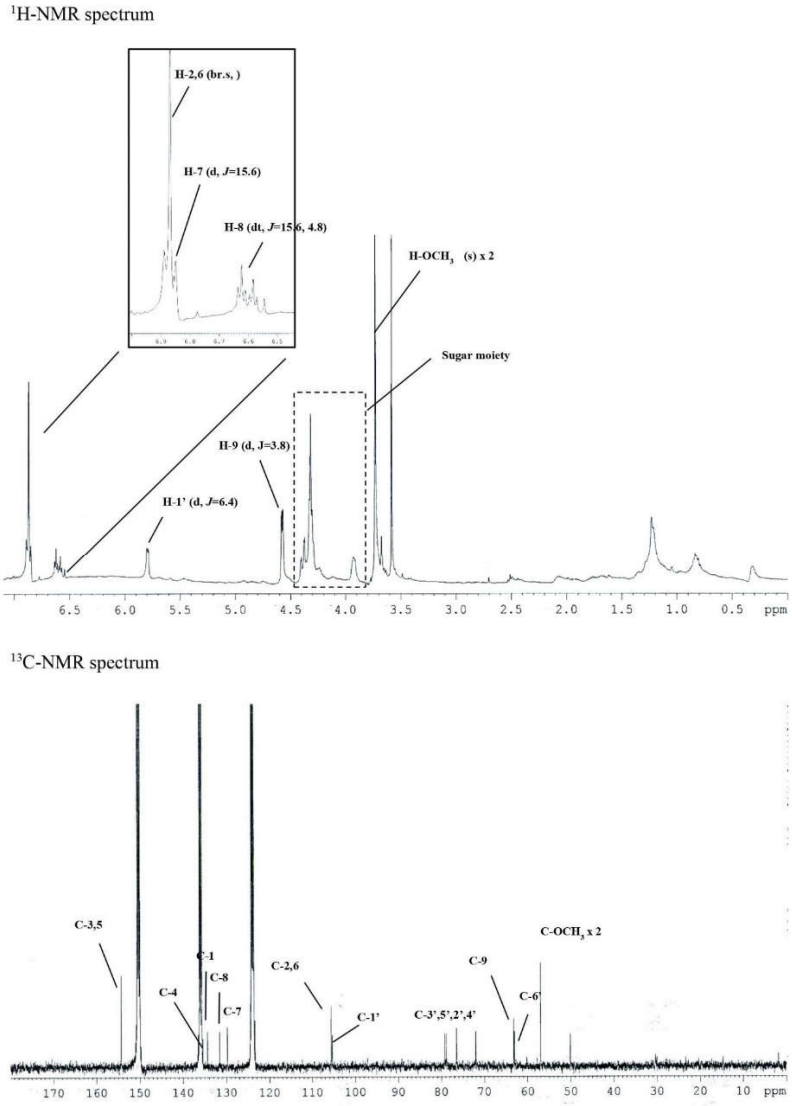

Figure 4. The ¹H-NMR and ¹³C-NMR spectrum of Compound 2 (10.4 mg).

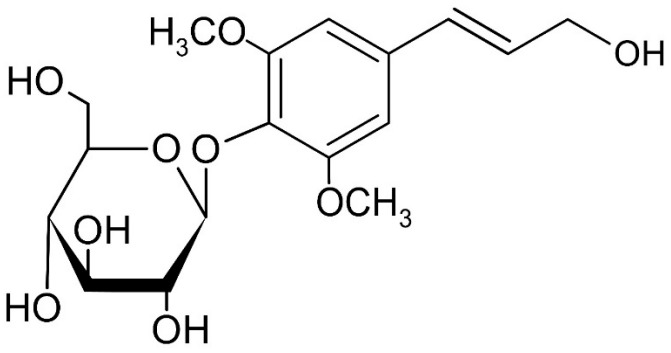

Figure 5. Chemical structure of the isolated syringin ($C_{17}H_{24}O_9$) from *S. neoserrata* Nakai.

Preprints (www.preprints.org) | NOT PEER-REVIEWED | Posted: 25 June 2023 doi:10.20944/preprints202306.1713.v1

3.3. PM_{10} Induces Cytotoxicity in and PGE_2 and PGD_2 Release from Keratinocytes

To examine whether airborne PM_{10} can cause cytotoxicity and inflammation, HaCaT cells were exposed to PM_{10} in vitro. PM_{10} treatments at 100 μg/mL for 48 h decreased the cell viability (Figure 6a). The conditioned cell culture media were used for determining the concentrations of PGE_2 and PGD_2. PGE_2 and PGD_2 production increased in the cells exposed to PM_{10} at 25 μg/mL for 48 h (Figure 6b,c). A concentration of 12.5 μg/mL was used in the experiment to keep PM10 within the non-toxic concentration range.

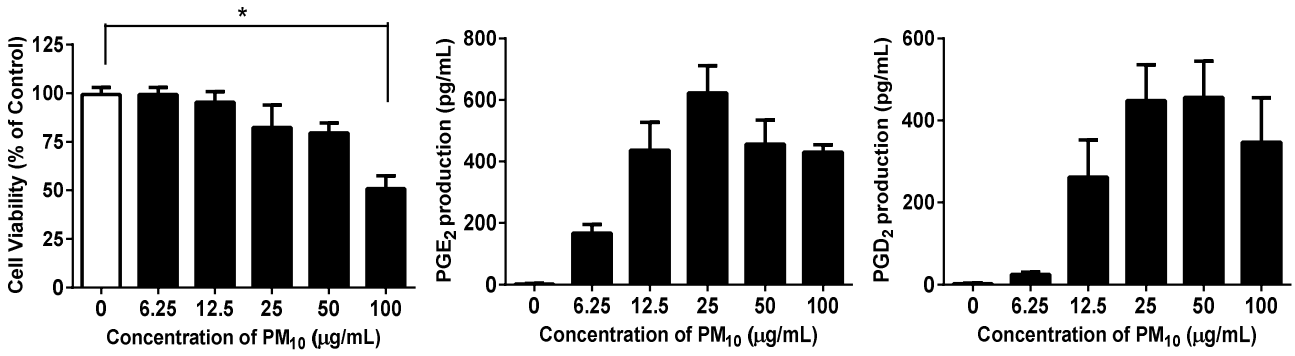

(a) (b) (c)

Figure 6. The impact of particulate matter with a diameter of less than 10 microns (PM10) on the viability and release of PGE2 and PGD2 in HaCaT keratinocytes was examined. The cells were exposed to different concentrations of PM10 for a duration of 48 hours in order to conduct the viability assay. (a) and the PGE_2 (b) and PGD_2 (c) release assays. Control cells were treated with saline. Data are presented as the mean ± standard deviation (SD) (n = 4). All treatments were compared with the controls using one-way analysis of variance (ANOVA) followed by Dunnett's test. * $p < 0.05$.

3.4. Effects of *S. neoserrata* Nakai Extracts on PM_{10}-Induced Cytotoxicity and PGE_2 and PGD_2 Release

To investigate whether the *S. neoserrata* Nakai extract had any effect on the viability of HaCaT keratinocytes, the cells were treated with various concentrations (10 to 200 μg/mL) of *S. neoserrata* Nakai extract for 48 hours. Our results confirmed that the viability of HaCaT keratinocytes was not affected by *S. neoserrata* Nakai extract at the concentrations and culture durations tested (Figure 7a). Next, in order to confirm the effect of the *S. neoserrata* Nakai extract on the inflammatory response of HaCaT cells, the keratinocytes were exposed to 12.5 μg/mL PM_{10} in the presence of 10 to 200 μg/mL *S. neoserrata* Nakai extract. The results indicate that the *S. neoserrata* Nakai extract inhibited PM_{10}-stimulated PGE_2 and PGD_2 release in a dose-dependent manner (Figure 7b,c).

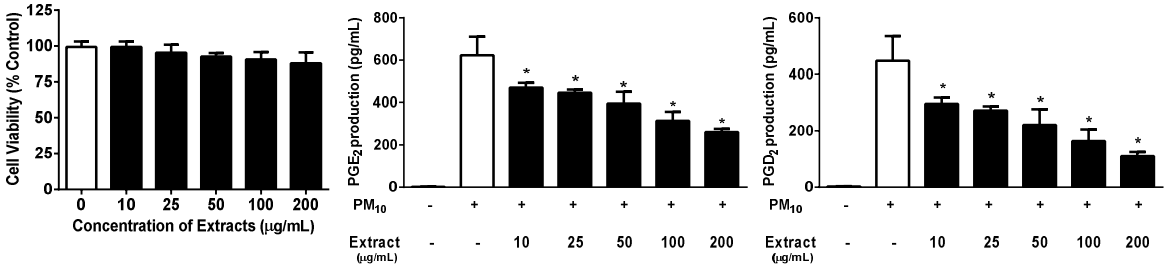

(a) (b) (c)

Figure 7. Effects of *S. neoserrata* Nakai extracts on the viability and the PGE_2 and PGD_2 release of HaCaT keratinocytes in response to PM_{10}. The cells were treated with 12.5 μg/mL PM_{10} in the presence of various concentrations of *S. neoserrata* Nakai extract for 48 h for the purposes of a viability assay (a) and PGE_2 (b) and PGD_2 (c) release assays. Data are presented as the mean ± SD (n = 4). All treatments were compared with the PM_{10}-only control using one-way ANOVA followed by Dunnett's test. * $p < 0.05$.

Preprints (www.preprints.org) | NOT PEER-REVIEWED | Posted: 25 June 2023 doi:10.20944/preprints202306.1713.v1

3.5. Effects of protocatechuic acid and syringin on PM_{10}-induced Keratinocyte Cytotoxicity and PGE_2 and PGD_2 Release

Protocatechuic acid showed a trend of decreasing HaCaT cell viability when added at concentrations between 30 and 100 μg/mL for 48 h (Figure 8a); however, the only statistically significant difference occurred at 100μg/mL protocatechuic acid. Syringin did not alter the viability when tested at concentrations of up to 20 μg/mL, though there was a trend for decreasing HaCaT cell viability at concentrations above this. In subsequent experiments both protocatechuic acid and syringin were used at 10 and 20 μg/mL concentrations in order to keep within the non-toxic concentration range. Syringin dose-dependently and significantly reduced the release of PGE_2 from keratinocytes exposed to 12.5 μg/mL PM_{10} (Figure 8d). On the other hand, protocatechuic acid dose-dependently and significantly reduced the release of PGD_2 from keratinocytes exposed to 50 μg/mL PM_{10} (Figure 8e). NAC (10 μg/mL) was used as a positive control antioxidant.

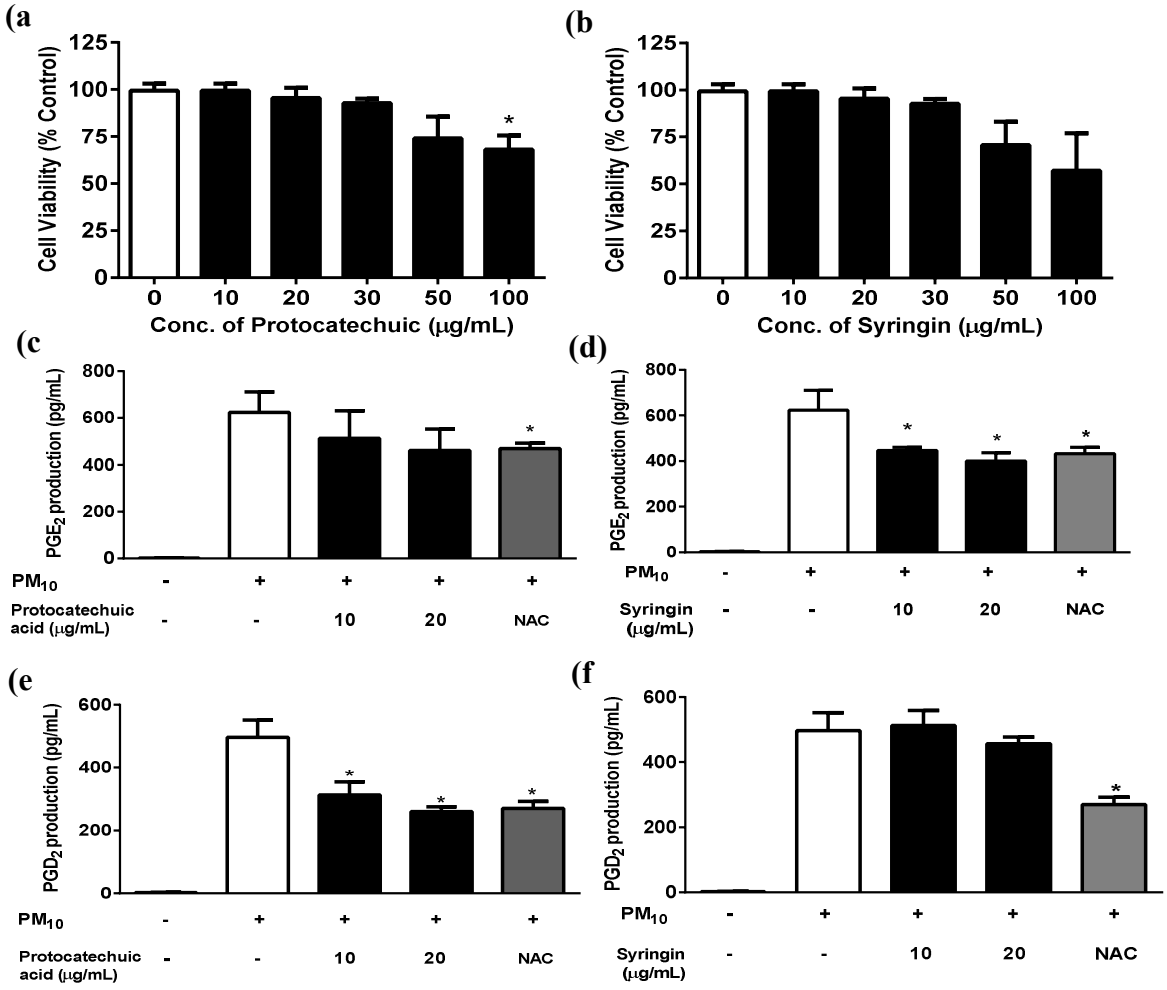

Figure 8. Effects of protocatechuic acid and syringin on PM_{10}-induced keratinocyte cytotoxicity and PGE_2 and PGD_2 release. HaCaT keratinocytes were treated with various concentrations of protocatechuic acid and syringin for 48 h, and the resulting cell viability was measured (a,b). Cells were treated with 50 μg/mL PM_{10} in the presence or absence of protocatechuic acid and syringin at the indicated concentrations for 48 h for the PGE_2 and PGD_2 release assays (c-f). NAC (10 μg/mL) was used as a positive control antioxidant in each assay. Data are presented as the mean ± SD (n = 4). All treatments were compared with the PM_{10}-only control using one-way ANOVA followed by Dunnett's test. * $p < 0.05$.

Preprints (www.preprints.org) | NOT PEER-REVIEWED | Posted: 25 June 2023 doi:10.20944/preprints202306.1713.v1

3.6. Effects of protocatechuic acid and syringin on PM_{10}-Induced ROS Production

Keratinocytes were treated with 12.5 μg/mL PM_{10} to induce oxidative stress, and the ability of protocatechuic acid and syringin to remove ROS was measured. The ROS removal ability of the *S. neoserrata* Nakai extract was assessed using DCF-DA, the green fluorescence being proportional to the amount of ROS present. When the HaCaT cells were treated with 12.5 μg/mL PM_{10}, the intracellular ROS levels were increased compared with the control group. Cells with PM_{10}-induced increased ROS were treated with *S. neoserrata* Nakai extract (100 and 200 μg/mL), protocatechuic acid (10 and 20 μg/mL), and syringin (10 and 20 μg/mL). Each treatment decreased PM_{10}-induced ROS in a concentration-dependent manner. This experiment confirmed that treatment with the protocatechuic acid and syringin derived from *S. neoserrata* Nakai extracts effectively reduced the intracellular ROS levels in HaCaT keratinocytes.

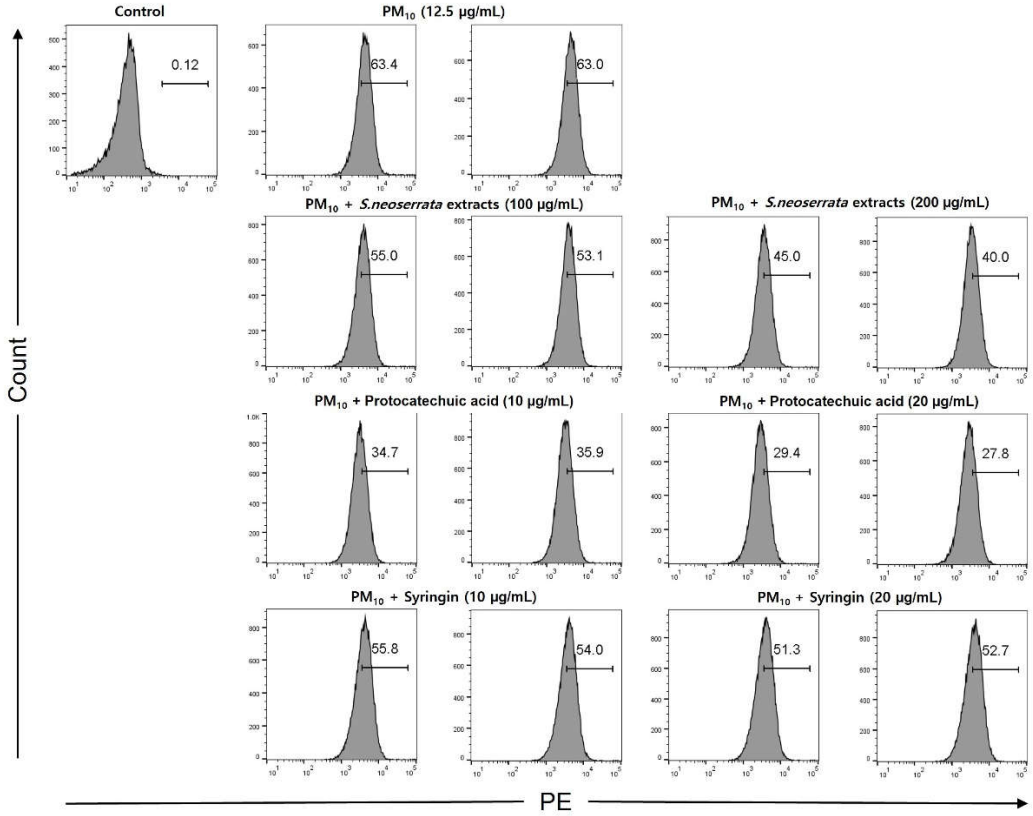

Figure 9. Effect of *S. neoserrata* Nakai extract, protocatechuic acid, and syringin on the PM_{10}-induced ROS production.

3.7. Effects of protocatechuic acid and syringin on the PM_{10}-Induced Gene Expression of the Enzymes Involved in the PGE_2 and PGD_2 Synthesis

Since the PM_{10}-induced release of PGE_2 and PGD_2 was attenuated by *S. neoserrata* Nakai extract, additional experiments were performed to determine the mRNA expression levels of the enzymes involved in PGE_2 and PGD_2 production. NAC (10 μg/mL) was also tested in the same manner at as a positive control antioxidant.

As the protocatechuic acid extracted from *S. neoserrata* Nakai extracts was more effective at inhibiting PGD_2 production, we aimed to investigate the mRNA expression levels of L-PGDS and H-PGDS, which are both involved in PGD_2 production, in response to protocatechuic acid. Treatment with 12.5 μg/mL PM_{10} increased the mRNA expression levels of L-PGDS, and these changes were greatly attenuated by protocatechuic acid treatment. Treatment with 10 μg/mL NAC resulted in a similar level of inhibition as that observed using 20 μg/mL protocatechuic acid (Figure 10). On the other hand, the H-PGDS expression increase induced by PM_{10} treatment was not attenuated by

Preprints (www.preprints.org) | NOT PEER-REVIEWED | Posted: 25 June 2023 doi:10.20944/preprints202306.1713.v1

protocatechuic acid. However, 10 μg/mL NAC did reverse the increase in H-PGDS expression (Figure 10).

The syringin extracted from *S. neoserrata* Nakai extracts was more effective in inhibiting PGE_2 production than other prostaglandins. Therefore, the correlation between the mRNA expression levels of the mPGES-1, mPGES-2, and cPGES (all involved in PGE_2 production) and treatment with syringin was investigated. Treatment with 50 μg/mL PM_{10} increased the expression of mPGES-1 at the mRNA level. However, these changes were greatly attenuated by treatment with 20 μg/mL syringin. A 10 μg/mL concentration of NAC suppressed the increased mPGES-1 expression to a similar level as 20 μg/mL syringin. PM_{10} treatment at 50 μg/mL did not increase the expression of mPGES-2 and cPGES at the mRNA level.

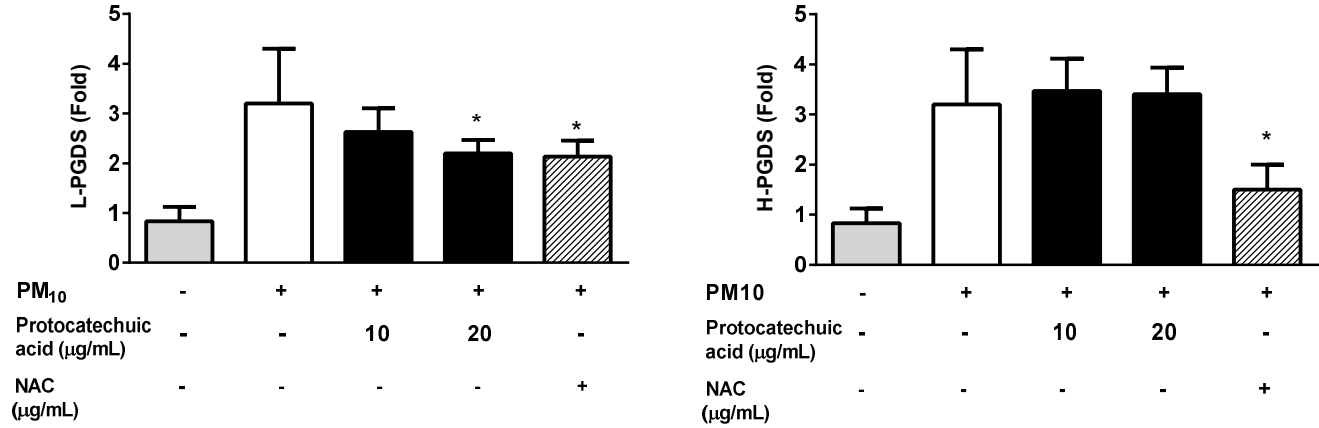

(a) (b)

Figure 10. Effects of protocatechuic acid on the PM_{10}-induced gene expression of the enzymes involved in the PGD_2 synthesis.

Cells were treated with 12.5 μg/mL PM_{10} for 24 h in the presence or absence of protocatechuic acid at the indicated concentrations in order to determine the mRNA expression of enzymes involved in PGD_2 synthesis (L-PGDS and H-PGDS). N-acetyl cysteine (NAC) was employed as a positive control antioxidant. All treatments were compared with the PM_{10}-only control using one-way ANOVA followed by Dunnett's test. * $p < 0.05$.

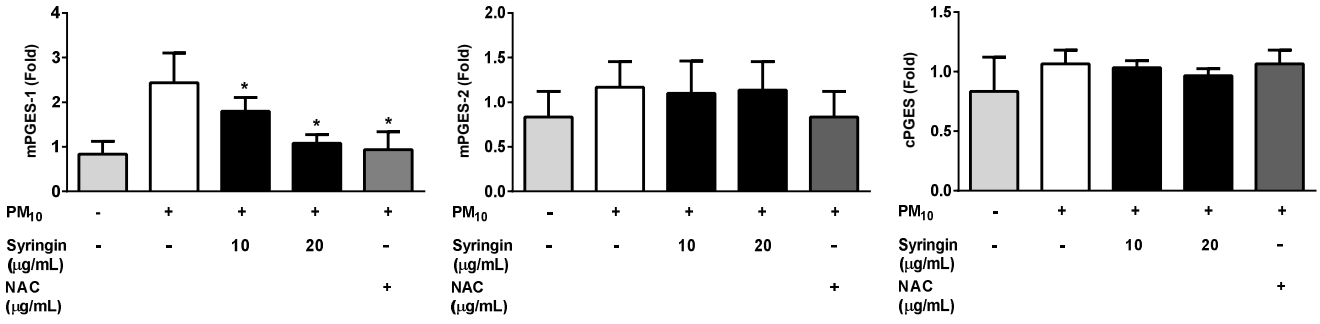

(a) (b) (c)

Figure 11. Effects of syringin on the PM_{10}-induced gene expression of the enzymes involved in the PGE_2 synthesis.

To examine the mRNA expression of enzymes associated with PGD_2 synthesis (L-PGDS and H-PGDS), cells were exposed to 12.5 μg/mL PM_{10} for 24 hours with or without protocatechuic acid at the specified concentrations. N-acetyl cysteine (NAC) was employed as a positive control antioxidant. All treatments were compared with the PM_{10}-only control using one-way ANOVA followed by Dunnett's test. * $p < 0.05$. μg/mL

Preprints (www.preprints.org) | NOT PEER-REVIEWED | Posted: 25 June 2023 doi:10.20944/preprints202306.1713.v1

4. Discussion

In the present paper, extracts of *S. neoserrata* Nakai that were previously unstudied were isolated and identified as protocatechuic acid (C7H6O4) and syringin (C17H24O9). This is the first report on a structural explanation and identification of the protocatechuic acid and syringin active compounds contained in *S. neoserrata* Nakai. The established prep-LC method proved to be simple, precise, and accurate. The protocatechuic acid identified in 3,4-dihydroxybenzoic acid has been previously found to play an important role in antioxidant activity [37]. The mass spectrum of the 3,4-dihydroxybenzoic acid identified the molecular ion [M-H]− at a m/z 153 atomic mass unit (amu) and a base peak [M-H-CO2]⁻ at m/z 108.9 amu.

In the present study, the *S. neoserrata* Nakai extracts served as the protective component against PM_{10} toxicity for HaCaT keratinocytes. The *S. neoserrata* Nakai extracts no more effectively attenuated PGE_2 and PGD_2 production in the cells exposed to varying concentrations of PM_{10} than NAC, which is a positive control antioxidant. The protocatechuic acid and syringin purified from *S. neoserrata* Nakai extracts also exhibited inhibitory activity against PM_{10}-induced PGE_2 and PGD_2 production.

Protocatechuic acid is present in a significant number of plants used in folk remedies, and it is a type of phenolic acid [38]. Protocatechuic acid has anti-inflammatory and antioxidant activity [39]. Lipocalin-type prostaglandin D synthase (L-PGDS) is from a group of secreted proteins that make up the lipocalin superfamily and which bind to lipophilic molecules [40]. L-PGDS is a monomeric protein present in several mammalian central nervous system tissues and the male genital organs; in addition, it is abundant in cerebrospinal fluid [41]. Hematopoietic prostaglandin D synthase (H-PGDS) is a member of the sigma-class of glutathione-S-transferases (GST). H-PGDS is expressed in various immune and inflammatory cells, such as mast cells and type 2 T lymphocytes [42,43]. L-PGDS and H-PGDS are involved in the production of prostaglandin D_2 (PGD_2), which is obtained from PGH_2 via isomerization [44]. The relationship between PGD_2 and inflammation is complex and not fully established. However, PGD_2 has been reported to contribute to allergic inflammatory reactions [45,46].

The results of our study show that treatment with protocatechuic acid significantly reduces PM_{10}-induced increases in L-PGDS in a concentration-dependent manner. A decrease in L-PGDS, which is one of the synthetases of PGD_2, ultimately causes a decrease in PGD_2. This finding suggests that protocatechuic acid may have a protective role in the inflammation and oxidative stress associated with PM_{10} exposure.

The synthesis of PGE_2 initiates by transforming membrane phospholipids into arachidonic acid with the assistance of phospholipase A2. Subsequently, arachidonic acid undergoes chemical reactions to form PGG_2, which further converts to PGH_2. These conversion processes are facilitated by the enzymes COX-1 and COX-2 [47]. Both COX isoforms can be detected in healthy human tissues and show increased expression in different disease states [48]. The transformation of PGH_2 into PGE_2 is facilitated by enzymes such as mPGES-1, mPGES-2, and cPGES [49], with mPGES-1 being the primary isoform responsible for heightened PGE_2 synthesis during inflammatory processes [50].

Syringin is a glucoside present in a variety of plant species (US, MAHADEVA RAO). It has also been extensively studied for potential therapeutic effects because of its antioxidant, anti-inflammatory, anticancer, and neuroprotective properties [51-54]. Our results demonstrate that elevated mPGES-1 in response to PM_{10} exposure was significantly suppressed by syringin treatment. This means that the synthesis of PGE_2 is ultimately inhibited. These results may mean that syringin has potential as a treatment for the adverse health effects of PM_{10} exposure. Further studies are required to investigate the mechanisms by which syringin exhibits PGE_2 inhibitory effects and to determine the safety and efficacy required for its clinical use.

The toxic elements present in airborne PM, such as heavy metals and polycyclic hydrocarbons, have pro-oxidative and pro-inflammatory effects on tissues, although the composition of PM varies depending on factors such as location, altitude, and season [55-57]. The exposure to PM_{10} triggers the generation of reactive oxygen species (ROS) through the aryl hydrocarbon receptor/NADPH oxidase-dependent pathway. Additionally, emerging research indicates that dual oxidase 2 is implicated in

ROS production in keratinocytes when exposed to PM [18,58-61]. Therefore, the use of antioxidants may help alleviate the negative skin reactions that result from exposure to PM.

Previous studies have demonstrated that various antioxidants, including NAC, can reduce the cellular ROS production induced by PM [62,63]. The ROS generated by PM can stimulate the MAPK family, which includes ERK, JNK and p38 kinase, along with the NF-κB signaling pathway. This activation subsequently triggers redox-sensitive transcription factors like AP-1 and NF-κB [14,64,65]. COX-2 mRNA expression is controlled by different transcription factors, including the cyclic-AMP response element binding protein and NF-κB, which become activated by various MAPKs and other protein kinases [66]. When keratinocytes are exposed to PM, it can stimulate MAPKs like ERK, p38 and JNK, resulting in the eventual expression of COX-2 [67]. The response to PM involves multiple redox-sensitive pathways that are involved in the regulation of PGE2 and PGD2 synthesis. It is suggested that the antioxidants present in *S. neoserrata* Nakai extracts, namely protocatechuic acid and syringin, may inhibit these various signaling pathways, thereby reducing the production of PGE_2 and PGD_2 in response to PM exposure. However, further research is necessary to confirm this concept and to evaluate the effectiveness of protocatechuic acid and syringin in vivo.

Acknowledgments: This work was supported by the academic research funds from the Catholic University of Pusan in 2021 and the National Research Foundation of Korea (NRF) grant funded by the Korea government (MSIT) (No. NRF-2022R1F1A1074419 and NRF-2022R1F1A1066041).

Conflicts of Interest: The authors declare no conflict of interest.

References

1. Krzyzanowski, M. WHO air quality guidelines for Europe. *Journal of Toxicology and Environmental Health, Part A* **2008**, *71*, 47-50.
2. Jia, Y.-Y.; Wang, Q.; Liu, T. Toxicity research of PM2. 5 compositions in vitro. *International journal of environmental research and public health* **2017**, *14*, 232.
3. Momtazan, M.; Geravandi, S.; Rastegarimehr, B.; Valipour, A.; Ranjbarzadeh, A.; Yari, A.R.; Dobaradaran, S.; Bostan, H.; Farhadi, M.; Darabi, F. An investigation of particulate matter and relevant cardiovascular risks in Abadan and Khorramshahr in 2014–2016. *Toxin reviews* **2019**, *38*, 290-297.
4. Shahriyari, H.A.; Nikmanesh, Y.; Jalali, S.; Tahery, N.; Zhiani Fard, A.; Hatamzadeh, N.; Zarea, K.; Cheraghi, M.; Mohammadi, M.J. Air pollution and human health risks: mechanisms and clinical manifestations of cardiovascular and respiratory diseases. *Toxin Reviews* **2022**, *41*, 606-617.
5. Dobaradaran, S.; Geravandi, S.; Goudarzi, G.; Idani, E.; Salmanzadeh, S.; Soltani, F.; Yari, A.R.; Mohammadi, M.J. Determination of cardiovascular and respiratory diseases caused by PM10 exposure in Bushehr, 2013. *Journal of Mazandaran university of medical sciences* **2016**, *26*, 42-52.
6. Bakke, J.V.; Wieslander, G.; Norback, D.; Moen, B.E. Eczema increases susceptibility to PM10 in office indoor environments. *Archives of Environmental & Occupational Health* **2012**, *67*, 15-21.
7. Jin, S.-P.; Li, Z.; Choi, E.K.; Lee, S.; Kim, Y.K.; Seo, E.Y.; Chung, J.H.; Cho, S. Urban particulate matter in air pollution penetrates into the barrier-disrupted skin and produces ROS-dependent cutaneous inflammatory response in vivo. *Journal of dermatological science* **2018**, *91*, 175-183.
8. Pan, T.-L.; Wang, P.-W.; Aljuffali, I.A.; Huang, C.-T.; Lee, C.-W.; Fang, J.-Y. The impact of urban particulate pollution on skin barrier function and the subsequent drug absorption. *Journal of dermatological science* **2015**, *78*, 51-60.
9. Ahn, K. The role of air pollutants in atopic dermatitis. *Journal of Allergy and Clinical Immunology* **2014**, *134*, 993-999.
10. Vierkötter, A.; Schikowski, T.; Ranft, U.; Sugiri, D.; Matsui, M.; Krämer, U.; Krutmann, J. Airborne particle exposure and extrinsic skin aging. *Journal of investigative dermatology* **2010**, *130*, 2719-2726.

11. Roberts, W.E. Pollution as a risk factor for the development of melasma and other skin disorders of facial hyperpigmentation-is there a case to be made? *Journal of Drugs in Dermatology: JDD* **2015**, *14*, 337-341.
12. Martic, I.; Jansen-Dürr, P.; Cavinato, M. Effects of air pollution on cellular senescence and skin aging. *Cells* **2022**, *11*, 2220.
13. Soeur, J.; Belaïdi, J.-P.; Chollet, C.; Denat, L.; Dimitrov, A.; Jones, C.; Perez, P.; Zanini, M.; Zobiri, O.; Mezzache, S. Photo-pollution stress in skin: Traces of pollutants (PAH and particulate matter) impair redox homeostasis in keratinocytes exposed to UVA1. *Journal of dermatological science* **2017**, *86*, 162-169.
14. Wang, J.; Huang, J.; Wang, L.; Chen, C.; Yang, D.; Jin, M.; Bai, C.; Song, Y. Urban particulate matter triggers lung inflammation via the ROS-MAPK-NF-κB signaling pathway. *Journal of thoracic disease* **2017**, *9*, 4398.
15. Xia, T.; Kovochich, M.; Nel, A. The role of reactive oxygen species and oxidative stress in mediating particulate matter injury. *Clin Occup Environ Med* **2006**, *5*, 817-836.
16. Park, S.-Y.; Byun, E.J.; Lee, J.D.; Kim, S.; Kim, H.S. Air pollution, autophagy, and skin aging: impact of particulate matter (PM10) on human dermal fibroblasts. *International journal of molecular sciences* **2018**, *19*, 2727.
17. Romani, A.; Cervellati, C.; Muresan, X.M.; Belmonte, G.; Pecorelli, A.; Cervellati, F.; Benedusi, M.; Evelson, P.; Valacchi, G. Keratinocytes oxidative damage mechanisms related to airbone particle matter exposure. *Mechanisms of Ageing and Development* **2018**, *172*, 86-95.
18. Lee, C.-W.; Lin, Z.-C.; Hu, S.C.-S.; Chiang, Y.-C.; Hsu, L.-F.; Lin, Y.-C.; Lee, I.-T.; Tsai, M.-H.; Fang, J.-Y. Urban particulate matter down-regulates filaggrin via COX2 expression/PGE2 production leading to skin barrier dysfunction. *Scientific reports* **2016**, *6*, 27995.
19. Gong, W.; Zhao, N.; Zhang, Z.; Zhang, Y.; Yan, L.; Li, J. The inhibitory effect of resveratrol on COX-2 expression in human colorectal cancer: A promising therapeutic strategy. *Eur Rev Med Pharmacol Sci* **2017**, *21*, 1136-1143.
20. Cianciulli, A.; Calvello, R.; Cavallo, P.; Dragone, T.; Carofiglio, V.; Panaro, M.A. Modulation of NF-κB activation by resveratrol in LPS treated human intestinal cells results in downregulation of PGE2 production and COX-2 expression. *Toxicology in Vitro* **2012**, *26*, 1122-1128.
21. Tsai, M.-H.; Hsu, L.-F.; Lee, C.-W.; Chiang, Y.-C.; Lee, M.-H.; How, J.-M.; Wu, C.-M.; Huang, C.-L.; Lee, I.-T. Resveratrol inhibits urban particulate matter-induced COX-2/PGE2 release in human fibroblast-like synoviocytes via the inhibition of activation of NADPH oxidase/ROS/NF-κB. *The International Journal of Biochemistry & Cell Biology* **2017**, *88*, 113-123.
22. Lee, C.-W.; Lin, Z.-C.; Hsu, L.-F.; Fang, J.-Y.; Chiang, Y.-C.; Tsai, M.-H.; Lee, M.-H.; Li, S.-Y.; Hu, S.C.-S.; Lee, I.-T. Eupafolin ameliorates COX-2 expression and PGE2 production in particulate pollutants-exposed human keratinocytes through ROS/MAPKs pathways. *Journal of ethnopharmacology* **2016**, *189*, 300-309.
23. Boo, Y.C. Can plant phenolic compounds protect the skin from airborne particulate matter? *Antioxidants* **2019**, *8*, 379.
24. Juliano, C.; Magrini, G.A. Cosmetic functional ingredients from botanical sources for anti-pollution skincare products. *Cosmetics* **2018**, *5*, 19.
25. Michalak, M. Plant-derived antioxidants: Significance in skin health and the ageing process. *International journal of molecular sciences* **2022**, *23*, 585.
26. Shakya, A.K. Medicinal plants: Future source of new drugs. *International journal of herbal medicine* **2016**, *4*, 59-64.

27. Süntar, I. Importance of ethnopharmacological studies in drug discovery: role of medicinal plants. *Phytochemistry Reviews* **2020**, *19*, 1199-1209.
28. Zhao, T.; Li, S.-J.; Zhang, Z.-X.; Zhang, M.-L.; Shi, Q.-W.; Gu, Y.-C.; Dong, M.; Kiyota, H. Chemical constituents from the genus Saussurea and their biological activities. *Heterocyclic Communications* **2017**, *23*, 331-358.
29. Mishra, A.P.; Saklani, S.; Sharifi-Rad, M.; Iriti, M.; Salehi, B.; Maurya, V.K.; Rauf, A.; Milella, L.; Rajabi, S.; Baghalpour, N. Antibacterial potential of Saussurea obvallata petroleum ether extract: A spiritually revered medicinal plant. *Cellular and Molecular Biology* **2018**, *64*, 65-70.
30. Fan, C.-Q.; Yue, J.-M. Biologically active phenols from Saussurea medusa. *Bioorganic & medicinal chemistry* **2003**, *11*, 703-708.
31. Lee, W.T.; Im, H.T. Saussurea grandicapitula W. Lee et HT Im (Compositae), a new species from the Taebaek mountains, Korea. *Korean Journal of Plant Taxonomy* **2007**, *37*, 387-393.
32. Lin, W.; Li, Z. Blueberries inhibit cyclooxygenase-1 and cyclooxygenase-2 activity in human epithelial ovarian cancer. *Oncology Letters* **2017**, *13*, 4897-4904.
33. Xu, J.; Wu, W.; Zhang, H.; Yang, L. Berberine alleviates amyloid β25-35-induced inflammatory response in human neuroblastoma cells by inhibiting proinflammatory factors. *Experimental and therapeutic medicine* **2018**, *16*, 4865-4872.
34. Molloy, E.; Morgan, M.; Doherty, G.; McDonnell, B.; O'Byrne, J.; Fitzgerald, D.; McCarthy, G. Microsomal prostaglandin E2 synthase 1 expression in basic calcium phosphate crystal-stimulated fibroblasts: role of prostaglandin E2 and the EP4 receptor. *Osteoarthritis and cartilage* **2009**, *17*, 686-692.
35. Zayed, N.; Li, X.; Chabane, N.; Benderdour, M.; Martel-Pelletier, J.; Pelletier, J.-P.; Duval, N.; Fahmi, H. Increased expression of lipocalin-type prostaglandin D 2 synthase in osteoarthritic cartilage. *Arthritis research & therapy* **2008**, *10*, 1-12.
36. Lee, J.-w.; Seok, J.K.; Boo, Y.C. Ecklonia cava extract and dieckol attenuate cellular lipid peroxidation in keratinocytes exposed to PM10. *Evidence-Based Complementary and Alternative Medicine* **2018**, *2018*.
37. Kakkar, S.; Bais, S. A review on protocatechuic acid and its pharmacological potential. *International Scholarly Research Notices* **2014**, *2014*.
38. Liu, R.H. Potential synergy of phytochemicals in cancer prevention: mechanism of action. *The Journal of nutrition* **2004**, *134*, 3479S-3485S.
39. Winter, A.N.; Brenner, M.C.; Punessen, N.; Snodgrass, M.; Byars, C.; Arora, Y.; Linseman, D.A. Comparison of the neuroprotective and anti-inflammatory effects of the anthocyanin metabolites, protocatechuic acid and 4-hydroxybenzoic acid. *Oxidative medicine and cellular longevity* **2017**, *2017*.
40. Flower, D.R. The lipocalin protein family: structure and function. *Biochemical journal* **1996**, *318*, 1-14.
41. Urade, Y.; Kitahama, K.; Ohishi, H.; Kaneko, T.; Mizuno, N.; Hayaishi, O. Dominant expression of mRNA for prostaglandin D synthase in leptomeninges, choroid plexus, and oligodendrocytes of the adult rat brain. *Proceedings of the National Academy of Sciences* **1993**, *90*, 9070-9074.
42. Tanaka, K.; Ogawa, K.; Sugamura, K.; Nakamura, M.; Takano, S.; Nagata, K. Cutting edge: differential production of prostaglandin D2 by human helper T cell subsets. *The Journal of Immunology* **2000**, *164*, 2277-2280.
43. Urade, Y.; Ujihara, M.; Horiguchi, Y.; Igarashi, M.; Nagata, A.; Ikai, K.; Hayaishi, O. Mast cells contain spleen-type prostaglandin D synthetase. *Journal of Biological Chemistry* **1990**, *265*, 371-375.
44. Kanaoka, Y.; Urade, Y. Hematopoietic prostaglandin D synthase. *Prostaglandins, leukotrienes and essential fatty acids* **2003**, *69*, 163-167.

45. Pettipher, R. The roles of the prostaglandin D2 receptors DP1 and CRTH2 in promoting allergic responses. *British journal of pharmacology* **2008**, *153*, S191-S199.
46. Satoh, T.; Moroi, R.; Aritake, K.; Urade, Y.; Kanai, Y.; Sumi, K.; Yokozeki, H.; Hirai, H.; Nagata, K.; Hara, T. Prostaglandin D2 plays an essential role in chronic allergic inflammation of the skin via CRTH2 receptor. *The Journal of Immunology* **2006**, *177*, 2621-2629.
47. Ueno, N.; Murakami, M.; Tanioka, T.; Fujimori, K.; Tanabe, T.; Urade, Y.; Kudo, I. Coupling between cyclooxygenase, terminal prostanoid synthase, and phospholipase A2. *Journal of Biological Chemistry* **2001**, *276*, 34918-34927.
48. Zidar, N.; Odar, K.; Glavac, D.; Jerse, M.; Zupanc, T.; Stajer, D. Cyclooxygenase in normal human tissues–is COX-1 really a constitutive isoform, and COX-2 an inducible isoform? *Journal of cellular and molecular medicine* **2009**, *13*, 3753-3763.
49. Mattila, S.; Tuominen, H.; Koivukangas, J.; Stenbäck, F. The terminal prostaglandin synthases mPGES-1, mPGES-2, and cPGES are all overexpressed in human gliomas. *Neuropathology* **2009**, *29*, 156-165.
50. Camacho, M.; Gerboles, E.; ESCUDERO, J.R.; Anton, R.; Garcia-Moll, X.; Vila, L. Microsomal prostaglandin E synthase-1, which is not coupled to a particular cyclooxygenase isoenzyme, is essential for prostaglandin E2 biosynthesis in vascular smooth muscle cells. *Journal of Thrombosis and Haemostasis* **2007**, *5*, 1411-1419.
51. Kim, B.; Kim, M.-S.; Hyun, C.-K. Syringin attenuates insulin resistance via adiponectin-mediated suppression of low-grade chronic inflammation and ER stress in high-fat diet-fed mice. *Biochemical and Biophysical Research Communications* **2017**, *488*, 40-45.
52. Lee, C.-H.; Huang, C.-W.; Chang, P.-C.; Shiau, J.-P.; Lin, I.-P.; Lin, M.-Y.; Lai, C.-C.; Chen, C.-Y. Reactive oxygen species mediate the chemopreventive effects of syringin in breast cancer cells. *Phytomedicine* **2019**, *61*, 152844.
53. Lall, N.; Kishore, N.; Binneman, B.; Twilley, D.; Van de Venter, M.; Plessis-Stoman, D.d.; Boukes, G.; Hussein, A. Cytotoxicity of syringin and 4-methoxycinnamyl alcohol isolated from Foeniculum vulgare on selected human cell lines. *Natural product research* **2015**, *29*, 1752-1756.
54. Tan, J.; Luo, J.; Meng, C.; Jiang, N.; Cao, J.; Zhao, J. Syringin exerts neuroprotective effects in a rat model of cerebral ischemia through the FOXO3a/NF-κB pathway. *International Immunopharmacology* **2021**, *90*, 107268.
55. Donaldson, K.; Stone, V. Current hypotheses on the mechanisms of toxicity of ultrafine particles. *Annali dell'Istituto superiore di sanitÃ* **2003**, *39*, 405-410.
56. Araujo, J.A.; Nel, A.E. Particulate matter and atherosclerosis: role of particle size, composition and oxidative stress. *Particle and fibre toxicology* **2009**, *6*, 1-19.
57. Brook, R.D.; Rajagopalan, S. Particulate matter, air pollution, and blood pressure. *Journal of the American Society of Hypertension* **2009**, *3*, 332-350.
58. Lee, I.-T.; Yang, C.-M. Role of NADPH oxidase/ROS in pro-inflammatory mediators-induced airway and pulmonary diseases. *Biochemical pharmacology* **2012**, *84*, 581-590.
59. Bedard, K.; Krause, K.-H. The NOX family of ROS-generating NADPH oxidases: physiology and pathophysiology. *Physiological reviews* **2007**, *87*, 245-313.
60. Lassègue, B.; Griendling, K.K. NADPH oxidases: functions and pathologies in the vasculature. *Arteriosclerosis, thrombosis, and vascular biology* **2010**, *30*, 653-661.
61. Seok, J.K.; Choi, M.A.; Ha, J.W.; Boo, Y.C. Role of dual oxidase 2 in reactive oxygen species production induced by airborne particulate matter PM10 in human epidermal keratinocytes. *Journal of the Society of Cosmetic Scientists of Korea* **2019**, *45*, 57-67.

 doi:10.20944/preprints202306.1713.v1

62. Choi, S.-M.; Lee, P.-H.; An, M.-H.; Yun-Gi, L.; Park, S.; Baek, A.R.; Jang, A.-S. N-acetylcysteine decreases lung inflammation and fibrosis by modulating ROS and Nrf2 in mice model exposed to particulate matter. *Immunopharmacology and Immunotoxicology* **2022**, *44*, 832-837.
63. Jin, L.; Ni, J.; Tao, Y.; Weng, X.; Zhu, Y.; Yan, J.; Hu, B. N-acetylcysteine attenuates PM2. 5-induced apoptosis by ROS-mediated Nrf2 pathway in human embryonic stem cells. *Science of The Total Environment* **2019**, *666*, 713-720.
64. Choi, M.-K.; Kim, J.; Park, H.-M.; Lim, C.-M.; Pham, T.-H.; Shin, H.Y.; Kim, S.-E.; Oh, D.-K.; Yoon, D.-Y. The DPA-derivative 11S, 17S-dihydroxy 7, 9, 13, 15, 19 (Z, E, Z, E, Z)-docosapentaenoic acid inhibits IL-6 production by inhibiting ROS production and ERK/NF-κB pathway in keratinocytes HaCaT stimulated with a fine dust PM10. *Ecotoxicology and Environmental Safety* **2022**, *232*, 113252.
65. Ain, N.U.; Qamar, S.U.R. Particulate matter-induced cardiovascular dysfunction: a mechanistic insight. *Cardiovascular Toxicology* **2021**, *21*, 505-516.
66. Klein, T.; Shephard, P.; Kleinert, H.; Kömhoff, M. Regulation of cyclooxygenase-2 expression by cyclic AMP. *Biochimica et Biophysica Acta (BBA)-Molecular Cell Research* **2007**, *1773*, 1605-1618.
67. Teng, W.-L.; Huang, P.-H.; Wang, H.-C.; Tseng, C.-H.; Yen, F.-L. Pterostilbene attenuates particulate matter-induced oxidative stress, inflammation and aging in keratinocytes. *Antioxidants* **2021**, *10*, 1552.